Applied Geochemistry 100 (2019) 143–151

Contents lists available at ScienceDirect

Applied Geochemistry

journal homepage: www.elsevier.com/locate/apgeochem

Signature of oxygen and sulfur isotopes of sulfate in ground and surface water reflecting enhanced sulfide oxidation in mine areas

Duk-Min Kim[a,b], Seong-Taek Yun[a,c,*], Sungmoon Yoon[a,b], Bernhard Mayer[c]

[a] *Department of Earth and Environmental Sciences and KU-KIST Green School, Korea University, Seoul, 02841, South Korea*
[b] *Institute of Mine Reclamation Technology, Mine Reclamation Corporation (MIRECO), Wonju, 26464, South Korea*
[c] *Department of Geoscience, University of Calgary, Calgary, Alberta, T2N 1N4, Canada*

ARTICLE INFO

Editorial handling by Prof. M. Kersten

Keywords:
Sulfide oxidation pathways
Sulfur and oxygen isotopes of sulfate
Hydrochemistry
Mine tailings and wastes
Ground and surface water in mine area

ABSTRACT

Aqueous geochemistry data together with sulfur and oxygen isotope ratios of minerals and dissolved sulfate in ground and surface water were assessed in six mining areas including five metalliferous mines and one coal mine in various regions in South Korea. The $\delta^{34}S_{sulfate}$ values effectively reflected characteristic sulfur isotopic ratios of minerals in each mine area, and the $\delta^{18}O_{sulfate}$ values of mining-affected water (adit water and leachate) were depleted than those of background water. A plot of $\delta^{18}O_{sulfate}$ values versus the logarithmic sulfate concentration revealed a good linear negative relationship ($R^2 = 0.78$) for 219 samples spanning six mines in different regions. The observed range of $\delta^{18}O_{sulfate}$ values spanned the region where most of oxygen is derived from molecular oxygen for samples with low sulfate concentrations and the region of 100% oxygen derived from water molecules when sulfate concentrations were highest. This suggests that enhanced sulfide oxidation by ferric iron incorporating water-derived oxygen exponentially increases sulfate concentrations in mining areas. In addition, the lower and upper limits of sulfate in the plot could be defined as the atmospheric sulfate input and saturation of gypsum, respectively. The observed relationship between $\delta^{18}O_{sulfate}$ and sulfate concentration based on field data can further be used for semi-quantitative interpretation of oxygen isotopic ratios of sulfate in mine areas in terms of pyrite oxidation pathways.

1. Introduction

Sulfur and oxygen isotopic geochemistry of sulfate has been very useful in tracing and interpreting sources, transport and transformations of sulfate in mine areas (Toran, 1987; van Everdingen and Krouse, 1988; Dold and Spangenberg, 2005; Butler, 2007; Nordstrom et al., 2007; Hubbard et al., 2009; Junghans and Tichomirowa, 2009; Tuttle et al., 2009; Gammons et al., 2010, 2013; Samborska and Halas, 2010; Yuan and Mayer, 2012; Zhang et al., 2015; Killingsworth et al., 2018). The dominant sulfide mineral in many mining areas is pyrite. Overall, the processes involved in the oxidation of pyrite can be expressed as shown in equations (1)–(3) (Singer and Stumm, 1970):

$$FeS_2 + 3.5O_2 + H_2O \rightarrow Fe^{2+} + 2SO_4^{2-} + 2H^+ \tag{1}$$

$$Fe^{2+} + H^+ + 0.25O_2 \rightarrow Fe^{3+} + 0.5H_2O \tag{2}$$

$$FeS_2 + 14Fe^{3+} + 8H_2O \rightarrow 15Fe^{2+} + 2SO_4^{2-} + 16H^+ \tag{3}$$

Oxidation by Fe^{3+} has been shown to oxidize pyrite 18 to 170 times more rapidly than O_2 (Nordstrom and Alpers, 1999). In addition, the oxidation rate can also be enhanced by up to 5 orders of magnitude by iron-oxidizing bacteria such as *Acidithiobacillus ferrooxidans* and *Leptospirillum ferrooxidans* which are chemolithoautotrophs (Nordstrom and Alpers, 1999), resulting in markedly elevated sulfate concentrations.

The oxygen isotope ratios of sulfate generated by pyrite oxidation can provide insights into the oxidation pathways, because theoretically as much as 87.5% of sulfate-oxygen is derived from molecular oxygen in the case of equation (1) (Singer and Stumm, 1970), whereas in the case of equation (3), up to 100% of sulfate-oxygen can be derived from the water molecule rather than dissolved molecular oxygen as pyrite oxidation is relatively vigorous and the resulting Fe^{3+} is relatively predominant in the zone of pyrite oxidation (Bottrell, 2007; Nordstrom et al., 2007). Hence, $\delta^{18}O_{sulfate}$ values of water can be effectively utilized as a tracer for the oxidation pathway of sulfide mineral.

Sulfur isotope ratios ($\delta^{34}S$) can also be used to identify sources of sulfate, especially if combined with oxygen isotope ratios of sulfate (Krouse and Mayer, 2000). In mining areas, oxidation of sulfide minerals and organic sulfur compounds (e.g. in coal mines) are often

---

[*] Corresponding author. Department of Earth and Environmental Sciences and KU-KIST Green School, Korea University, Seoul, 02841, South Korea.
E-mail address: styun@korea.ac.kr (S.-T. Yun).

https://doi.org/10.1016/j.apgeochem.2018.11.018
Received 10 August 2018; Received in revised form 18 November 2018; Accepted 19 November 2018

predominant, while in surrounding areas mineralization of soil organic sulfur, dissolution of primary sulfate minerals such as gypsum and anhydrite, use of fertilizer, or atmospheric sulfate deposition constitute sources of sulfate that often have distinct isotopic compositions (Mayer, 2005). In addition, $\delta^{34}S_{sulfate}$ and $\delta^{18}O_{sulfate}$ may increase due to bacterial sulfate reduction (BSR), and oxygen isotope may also be exchanged between sulfite and ambient water during BSR (Betts and Voss, 1970; Krouse et al., 1991; Hubbard et al., 2009). Hence, careful evaluation of S and O isotope fractionation effects is required if the isotopic composition of sulfate is used for identification of sources of dissolved sulfate in aqueous systems.

Several previous studies have examined the $\delta^{18}O_{sulfate}$ values from various mining areas over the world (Taylor et al., 1984a; van Everdingen et al., 1985; Toran, 1987; Bottrell, 2007; Nordstrom et al., 2007; Sun et al., 2017; Migaszewski et al., 2018). Taylor et al. (1984a) showed microbial enhancement of pyrite oxidation in the West Shasta district of northern California, USA; van Everdingen et al. (1985) investigated the proportions of water-derived oxygen in sulfate in the Paint Pots in Kootenay National Park, British Columbia, Canada; Bottrell (2007) has examined the $\delta^{18}O_{sulfate}$ values to distinguish water bodies affected by mining from those affected by acid rain in the Xingwen karst aquifer in Sichuan, China; and from a 15 km-wide region of the Animas River Watershed, Colorado, USA, Nordstrom et al. (2007) have reported that sulfate in water from areas without mines tended to have slightly higher (by about 2–3‰) $\delta^{18}O$ values than sulfate in water from mining areas. Those studies using $\delta^{18}O_{sulfate}$ values were conducted based on a limited range of investigation areas often restricted to one specific ore deposit, and hence did not sufficiently reveal a significant relationship between sulfate concentrations and the oxygen isotope ratios of sulfate. In addition, most of the previously reported studies and experiments were conducted in environments of low pH where ferric iron can be present at high concentrations. In contrast, this study was conducted using a large dataset (n = 219) of dual S—O isotopes of sulfate from six different mining areas in various regions of South Korea, where surface and ground water often have neutral to acidic pH values. The status of water contamination in the mining areas of this study was evaluated by Kim et al. (2017) through hydrochemical investigations.

The main objectives of this study were: 1) to confirm the relationship between $\delta^{18}O_{sulfate}$ and sulfate concentration in various nationwide mine areas with understanding the origin of oxygen in generated dissolved sulfate, and 2) to understand factors controlling $\delta^{18}O_{sulfate}$ and $\delta^{34}S_{sulfate}$. The findings of this study will be useful for better interpreting sulfide oxidation pathways.

2. Methods

2.1. Study area

For this study, five abandoned metalliferous mines (Sambo, Buddeun, Samgwang, Gomyeong and Dongbo) and one coal mine under operation (Sangdeok) were selected throughout South Korea (Fig. 1). The Sambo mine in the Gyeonggi-do province was one of the largest producers of Pb and Zn, and the Sangdeok mine in the Gangwon-do province is a representative anthracite coal mine under operation in South Korea. A large-sized Au—Ag mine with huge tailings containing arsenic (Samgwang in the Chungcheongnam-do province) and three smaller Au—Ag mines (Buddeun in the Gyeongsangbuk-do province, Gomyeong and Dongbo in the Gangwon-do province) were also included for this study.

Types of ore and characteristics of contamination sources are summarized in Table 1. More details on the studied mines are available from Kim et al. (2017). Most of the six mines were abandoned between late 1980s and 1990s except the Sangdeok coal mine under operation. In the Sambo Pb—Zn—Ba (barite) mine, Pb and Zn were major products with minor amounts of Ba and Ag. There are two dumps of tailings (tailing dumps #1 and #2 with the horizontal extent of 51,345 m^2 and 18,249 m^2, respectively) located in two different catchment areas (Fig. 2a). Leachates are generated from each dump. In particular, the leachate from tailing dump #1 is flowing out to the land surface contaminating downstream paddy fields. A drainage is flowing out through an abandoned mine adit near the tailing dump #2 and then joins the leachate from dump #2 (Kim et al., 2017).

The Buddeun Au—Ag—Cu mine consists of hydrothermal quartz veins in granitic rocks. Major ore minerals are chalcopyrite, sphalerite,

Fig. 1. Locations of six mines for survey in South Korea.

Table 1
Types of ore and characteristics of contamination sources in studied mines.

Name	Operation period	Province	Ore	Contamination factor	
				Source	Element
Sambo	1956–1991	Gyeonggi	Pb, Zn	Tailings, Adit water	Mn, Zn
Buddeun	1915–1989	Gyeongbuk	Au, Ag, Cu	Tailings, Adit water	Mn, Zn
Samgwang	1928–1996	Chungnam	Au, Ag, Pb, Zn	Tailings, Adit water	As
Sangdeok	Under operation	Gangwon	Coal	Waste rock	Al
Gomyeong, Dongbo	1978–1993	Gangwon	Au, Ag	Tailings, Adit water	As, Mn

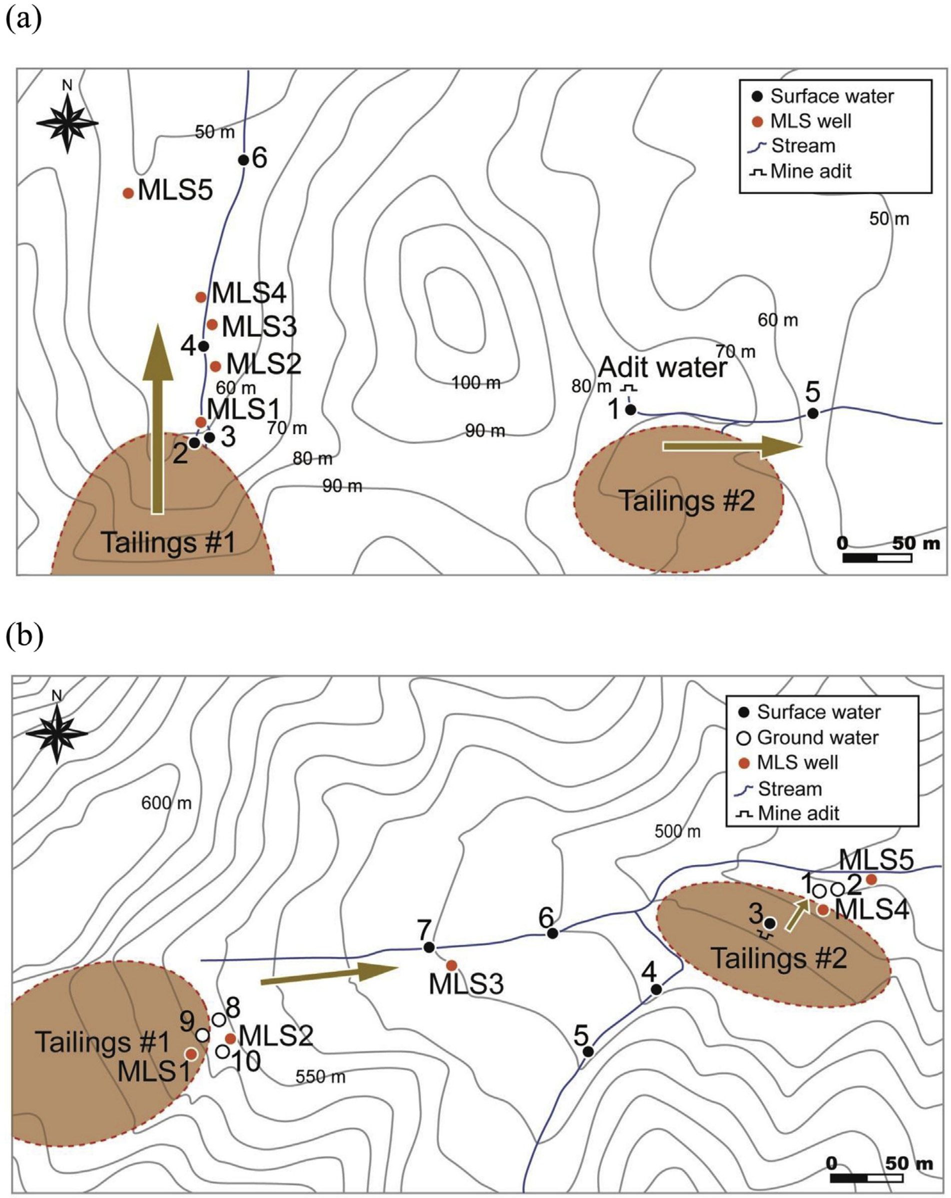

Fig. 2. Topography map, sampling locations, and contamination sources in (a) Sambo and (b) Buddeun mine (modified after Kim et al., 2017).

pyrite, arsenopyrite, galena, electrum and native silver (Park et al., 1988). Major sources of water contamination are two large tailing dumps (#1 and #2; Fig. 2b). There are groundwater boreholes (No. 1, 2, 8, 9 and 10) in front of the two tailing dumps, and a small creek at downstream (No. 6 and 7). There also is a small open channel (No. 4 and 5) beside the tailing dump #2 (Kim et al., 2017). The mine drainage flowing out from a mine adit (No. 3) soon seeps into the tailing dump #2.

Ores of the Samgwang Au—Ag mine occur as massive hydrothermal quartz veins in Precambrian gneiss (Lee and Hueley, 1973; Jeong et al., 1995). Major ore minerals are arsenopyrite, pyrite, sphalerite, chalcopyrite, galena with subordinate pyrrhotite, marcasite, electrum and argentite (Lee et al., 1998). There are two tailing dumps and two mine adits (No. 1 and 2) which discharge mine drainage (Fig. 3a). The drainages from the adits join a small stream (No. 3 and 4); the stream water flows into a pipeline after No. 4 and then seeps out again at No. 7. Tailing dump #1 discharges leachate as surface drainages (No. 5 and 8), while leachate from the tailing dump #2 does not appear on the land surface to infiltrate into subsurface (Kim et al., 2017).

The Gomyeong and Dongbo mines were the producers of Au and Ag from hydrothermal quartz veins in Precambrian gneiss. Major ore minerals include galena, sphalerite, chalcopyrite, pyrite and arsenopyrite (Kim et al., 1994). Both the mine adit water (flow rate: 36.0–86.4 $m^3 d^{-1}$) and the subsurface leachate from the tailing dump affect a stream near the Gomyeong mine (MIRECO, 2009). The Dongbo mine also shows a small amount of discharge ($< 3 m^3 d^{-1}$) from the adit and the tailing dump (Fig. 3b; Kim et al., 2017).

In the area of the Sangdeok coal mine under operation, pyrite-bearing anthracite seams and meta-sedimentary rocks of Permian age are the sources of acid mine drainage (AMD). A huge waste rock dump with the horizontal extent of ~100,000 m^2 discharges leachate (No. 5 in Fig. 4) and there are also stagnant leachates (No. 3 and 4). The leachates infiltrate into underground and seeps out again at a small stream ca. ~200 m away from the waste rock dump (No. 2). Immediately after the discharge into the stream, white precipitates of aluminum hydroxides are formed (Kim et al., 2017).

2.2. Field investigations and water sampling

A reconnaissance regional survey was conducted in March 2013 at

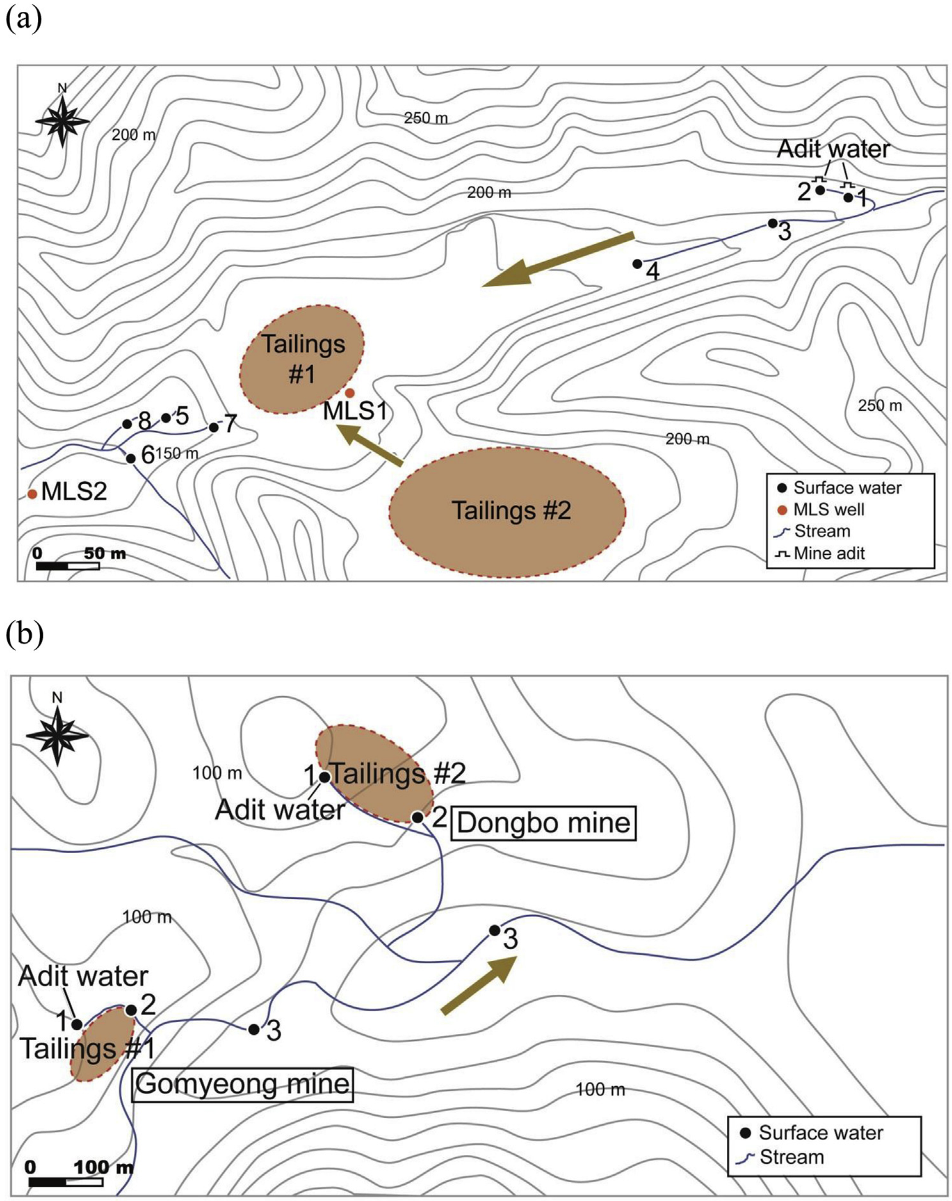

Fig. 3. Topography map, sampling locations, and contamination sources in (a) Samgwang mine and (b) Gomyeong and Dongbo mines (modified after Kim et al., 2017).

all the six mines to take representative water samples. The samples consisted mostly of surface water (n = 33) but also included seven groundwater samples (1, 2, 8, 9, 10, 12, 13) at Buddeun mine (Fig. 2b; Samples 12 and 13 were collected at a downstream village). Background surface water samples were also obtained from mining-unaffected separate catchment areas (Figs. 2–4). A total of 40 locations were chosen for water sampling for a reconnaissance survey.

To further examine the vertical and horizontal variations of groundwater chemistry, 12 multilevel samplers (MLS) were installed in the Sambo, Buddeun and Samgwang mine (five at Sambo, five at Buddeun and two at Samgwang) between late May and early June of 2013 (Figs. 2–4). Boreholes for the MLS were installed by rotary drilling down to ca. 20–30 m from the land surface. Immediately after the drilling, tubes and pipes were inserted into each borehole and then sand was used as a backfill material.

After the stabilization period for one month, sampling from MLS wells was conducted in July (the rainy season) and October (the dry season) of 2013. A total of 85 and 93 samples were collected in July and October, respectively, from twelve MLS wells using a peristaltic pump (Cole-Parmer Inc., USA). Prior to sampling, each sampling depth was purged until electric conductivity (EC) stabilized. Two groundwater samples at a separate catchment area ("background") and an adit water sample were additionally collected in the Sambo mine, and three groundwater samples were collected at 500–800 m downstream from the tailing dump #1 of the Samgwang mine at the time of sampling for MLS. Ore samples at all of the six mines were collected to analyze sulfur (for sulfides) and oxygen (for barite) isotope ratios.

Field parameters of water samples were measured using portable meters; Eh and pH using Orion model 290A, EC and temperature using Orion model 130A, and DO using Orion model 835A. Alkalinity (as HCO_3^-) was also determined in the field by volumetric titration using 0.05 N HNO_3. Dissolved sulfide was also determined in the field using a portable colorimeter (model HACH DR-890) following the methylene blue method (Cline, 1969).

Samples with each volume of 4 L were also collected for analyses of sulfur and oxygen isotope ratios of dissolved sulfate. After lowering the pH of the sample solutions to 3–4 using concentrated HCl to prevent precipitation of $BaCO_3$, $BaCl_2 \cdot 2H_2O$ was added to the filtered water

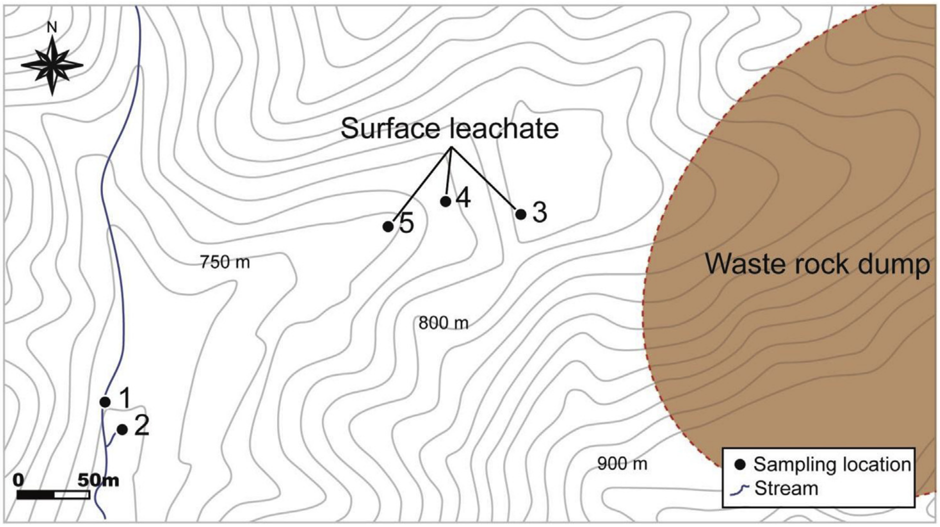

Fig. 4. Topography map, sampling locations, and contamination sources in Sangdeok coal mine (modified after Kim et al., 2017).

sample to precipitate sulfate as $BaSO_4$ in the field (Clark and Fritz, 1997).

2.3. Chemical and isotopic analysis

Collected water samples were filtered through a 0.45 μm pore size membrane and then immediately transferred into 60 ml high density polyethylene (HDPE) bottles which were pre-cleaned with the filtered samples in the field. The samples for the analysis of cations were preserved by adding a few drops of concentrated HNO_3 to keep the pH < 2. Sample bottles for the analysis of cations, anions and dissolved organic carbon (DOC) were completely filled with water and capped with an elastic laboratory film to avoid air contact and then stored in an ice box or refrigerator at 4 °C until analysis.

Concentrations of dissolved major cations (Ca, Mg, Na, K) were analyzed by an Inductively Coupled Plasma Atomic Emission Spectrometer (ICP-AES, Optima 3000XL, Perkin Elmer) at the Center for Mineral Resources Research (CMR), Korea University. Concentrations of other metals were analyzed by an Inductively Coupled Plasma Mass Spectrometer (ICP-MS, Perkin Elmer) at the Korea Basic Science Institute (KBSI) at Seoul. Anions were measured by ion chromatography (DX-120, Dionex) at CMR. Relative standard deviations (RSD) were generally below 5% of the measured value for ICP-AES, ICP-MS and ion chromatography. DOC was determined by a Total Organic Carbon analyzer (Sievers 5310C, General Electric) at the National Instrumentation Center for Environmental Management (NICEM) in Seoul National University. RSD was below 1% of the measured value for the DOC analyses. Geochemical modeling to calculate saturation indices (SI) was conducted using PHREEQC (Parkhurst and Appelo, 2015).

Precipitated $BaSO_4$ samples were recovered in the laboratory by 0.45 μm membrane filtration, and subsequently washed thoroughly with deionized water. The precipitates were then dried at room temperature. To obtain sulfur and oxygen isotope ratios of sulfate, the dried $BaSO_4$ samples were converted to SO_2 in an elemental analyzer and CO in a pyrolysis reactor, respectively, and analyzed by an isotope ratio mass spectrometer in continuous-flow mode in the Isotope Science Laboratory (ISL) at the University of Calgary (Alberta, Canada). The analytical results were reported as $\delta^{34}S$ relative to the Vienna Canyon Diablo Troilite (V-CDT) standard. The international reference materials NBS 127 ($\delta^{34}S = 21.1 \pm 0.4‰$, $\delta^{18}O = 9.3 \pm 0.4‰$), IAEA SO5 ($\delta^{34}S = 0.5 \pm 0.2‰$, $\delta^{18}O = 12.0 \pm 0.2‰$), IAEA SO6 ($\delta^{34}S = -34.1 \pm 0.2‰$, $\delta^{18}O = -11.0 \pm 0.2‰$) and several internal laboratory standards were used to ensure accurate measurements (Gonfiantini et al., 1995; Coplen et al., 2002). Analytical precisions were ± 0.3‰ for $\delta^{34}S$ and ± 0.5‰ for $\delta^{18}O$ of sulfate, respectively.

Sulfide minerals were physically separated from the collected ore and rock samples for chemical analysis, while tailings were processed in the bulk form. The rocks/tailings and ore samples were crushed and then pulverized using a ball mill and an agate mortar, respectively. To obtain sulfur isotope ratios of sulfide minerals, SO_2 was produced for analysis by reacting the sulfide mineral with an oxidant at elevated temperatures (1000–1200 °C) under vacuum (Holt and Engelkemeier, 1970; Haur et al., 1973; Coleman and Moore, 1978), and analyzed by an isotope ratio mass spectrometer in continuous-flow mode in the ISL at the University of Calgary. Sulfur and oxygen isotope ratios of barite ore samples were determined by the same procedure used for barium sulfate generated from other water samples. Analytical precisions were ± 0.3‰ for $\delta^{34}S$ and ± 0.5‰ for $\delta^{18}O$, respectively.

3. Results and discussion

3.1. Sulfur and oxygen isotopes of minerals

$\delta^{34}S$ of sulfide minerals at each mine and $\delta^{34}S$ and $\delta^{18}O$ of barite from the Sambo mine are presented in Table 2. Sulfide minerals

Table 2
$\delta^{34}S$ values of major minerals collected from studied mines and the $\delta^{18}O_{sulfate}$ values of barite from the Sambo mine.

Mine	Mineral	$\delta^{34}S$	$\delta^{18}O$
Sambo	Sphalerite (ZnS)	−5.6	–
	Galena (PbS)	−5.4	–
	Barite ($BaSO_4$)	18.0	4.3
	Barite (Kim et al., 1995)	15.7 to 17.2	2.4 to 3.9
	Sphalerite, galena, chalcopyrite (Kim et al., 1995)	−3.9 to 13.5	–
Buddeun	Pyrite (FeS_2)	6.7	–
	Sphalerite (ZnS)	6.4	–
Samgwang	Arsenopyrite (FeAsS)	3.9	–
	Arsenopyrite, sphalerite, chalcopyrite, galena (Moon, 1986; Yoo et al., 2002)	−0.5 to 5.2	
Sangdeok	Sedimentary pyrite (FeS_2)	−9.5	–
	Hydrothermal pyrite (FeS_2)	7.1	–
Gomyeong	Pyrite (FeS_2)	6.6	–
Dongbo	Pyrite (FeS_2)	7.0	–
	Sphalerite (ZnS)	5.6	–
	Galena (PbS)	5.7	–

(sphalerite and galena) found in the Sambo mine have $\delta^{34}S$ between −5.6 and −5.4‰ (avg. −5.5‰). Although pyrite was not analyzed at the mine, $\delta^{34}S$ of pyrite was assumed to be similar with that of sphalerite or galena, because they formed from similar hydrothermal fluids (So et al., 1984). In contrast, a sulfate mineral (barite) exhibited significantly higher $\delta^{34}S$ of 18.0‰ with $\delta^{18}O$ of 4.3‰. Sphalerite and pyrite collected at the tailing dump #2 of the Buddeun mine had $\delta^{34}S$ of 6.4‰ and 6.7‰ (avg. 6.6‰), respectively. An arsenopyrite from a rock sample in the Samgwang mine had $\delta^{34}S$ of 3.9‰, and which is similar with reported $\delta^{34}S$ ranges of arsenopyrite, sphalerite, galena, chalcopyrite and pyrite in the mine (3.3–5.2‰, 2.4–5.1‰, −0.5–3.0‰, 2.1–4.1‰ and 3.6–4.2‰, respectively) by Moon (1986) and Yoo et al. (2002). $\delta^{34}S$ of pyrite at the Gomyeong mine was 6.6‰, and that of pyrite, sphalerite and galena at the Dongbo mine were 7.0‰, 5.6‰ and 5.7‰, respectively. $\delta^{34}S$ of sedimentary pyrite (−9.5‰) was far less than that of hydrothermal pyrite (7.1‰) in the Sangdeok coal mine, and most of the pyrite found in the waste rocks were sedimentary origin.

3.2. Sulfur and oxygen isotopes in dissolved sulfate

$\Delta^{34}S_{sulfate\text{-}sulfide}$ and oxygen isotope ratios of the water samples from six mines were plotted together with classification of leachate/downstream, the deepest depths of MLS with low $\delta^{34}S_{sulfate}$ values (at 20 m of MLS5 in Sambo mine, at 20 m of MLS3 and at 18 and 20 m of MLS4 in Buddeun mine, and at 13, 16 and 20 m of MLS2 in Samgwang mine), adit water/downstream, and background water (Fig. 5). The differences between $\delta^{34}S$ of dissolved sulfate and that of sulfide minerals ($\Delta^{34}S_{sulfate\text{-}sulfide}$) were used in order to evaluate variation of $\delta^{34}S_{sulfate}$ with average $\delta^{34}S$ of intrinsic sulfide minerals at each mine.

There can be several factors controlling $\delta^{34}S_{sulfate}$ and $\delta^{18}O_{sulfate}$ including different sources (metal sulfides, organic soil, fertilizers), bacterial sulfate reduction, and dissolution of sulfate minerals. There was little evidence for bacterial sulfate reduction except for very few samples; the concentration of dissolved sulfide was generally below 0.1 mg l^{-1} except at 20 m depth of MLS3 at the Buddeun mine in July, and the concentration of DOC was mostly < 5 mg l^{-1}, indicating a lack of suitable reducing agents. In addition, primary evaporites were not present in geologic units of the study areas, although there is a possibility of precipitation of secondary gypsum at some MLS samples from Buddeun mine, which exhibited positive SI with respect to gypsum (see Table S1). Even though the precipitation and dissolution of secondary gypsum occur, isotopic composition of sulfur and oxygen in dissolved sulfate would be negligibly altered (Thode and Monster, 1965; Holser and Kaplan, 1966; Lloyd, 1968; Raab and Spiro, 1991; Hoefs, 2004).

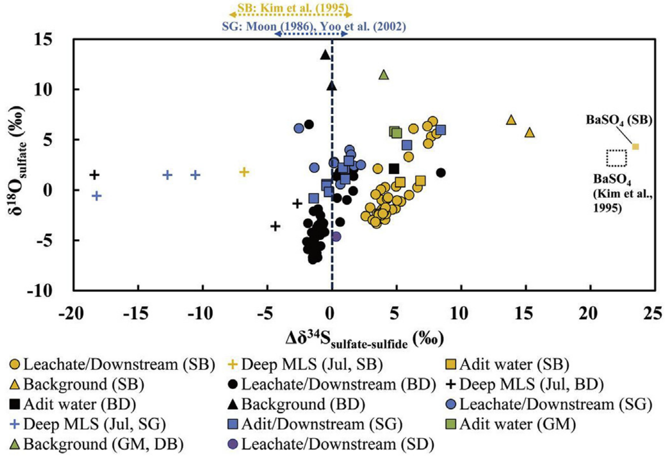

Fig. 5. Relationship between $\Delta\delta^{34}S_{sulfate\text{-}sulfide}$ and $\delta^{18}O_{sulfate}$ from regional and MLS surveys (SB: Sambo, BD: Buddeun, SG: Samgwang, GM: Gomyeong, DB: Dongbo, SD: Sangdeok). Isotopic values for barite from Sambo mine were also indicated.

Most of leachate and adit water had relatively low $\delta^{18}O_{sulfate}$ values, while background water samples (plotted as triangles) had sulfate with high $\delta^{18}O_{sulfate}$ values. In addition, most of the downstream water samples that were affected by leachate and/or adit water showed higher $\delta^{18}O_{sulfate}$ values than leachate and/or adit water, but lower values than background water. $\Delta^{34}S_{sulfate\text{-}sulfide}$ of most of the water samples were near 0‰, although Sambo mine suggests an effect from sulfate mineral (barite) dissolution with higher $\delta^{34}S_{sulfate}$, and limited samples from Gomyeong and Dongbo mine showed discrepancy ($\Delta^{34}S_{sulfate\text{-}sulfide}$) of about +5‰. Sulfur isotope fractionation during oxidation of sulfides to sulfate has been reported to be not more than a few per mil by several authors (Field, 1966; Taylor et al., 1984b; Toran and Harris, 1989; Heidel and Tichomirowa, 2011a; Balci et al., 2012). Reported enrichment factors for sulfate from pyrite ($\varepsilon^{34}S_{sulfate\text{-}FeS2}$) are −0.7‰ and −0.8‰ (Heidel and Tichomirowa, 2011a; Balci et al., 2007); $\varepsilon^{34}S_{sulfate\text{-}ZnS}$ for sphalerite are between 0‰ and −3.1‰ (Balci et al., 2012; Heidel et al., 2011); $\varepsilon^{34}S_{sulfate\text{-}PbS}$ for galena are between −0.1‰ and −4.0‰ (Heidel and Tichomirowa, 2011b); and $\varepsilon^{34}S_{sulfate\text{-}CuFeS2}$ for chalcopyrite are −0.5‰ and −3.8‰ (Thurston et al., 2010). Those enrichment factors are in accordance with the observed isotopic differences ($\Delta\delta^{34}S_{sulfate\text{-}sulfide}$) except the deepest MLS samples in rainy season (July). These exceptional samples were indicated as crosses in three mines, and all showed distinctly lower $\Delta^{34}S_{sulfate\text{-}sulfide}$ values with $\delta^{34}S_{sulfate}$ between −11.78 and −14.31‰. If "secondary" sulfides formed by sulfate reduction were present and oxidized, they might generate depleted sulfur isotope of sulfate. However, the number of the exceptional samples is limited and additional investigation would be necessary to elucidate the origin and mechanism.

3.3. Relationship between concentration and oxygen isotope of sulfate

Concentrations of dissolved sulfate (in logarithmic scale) from regional and MLS surveys were plotted against $\delta^{18}O_{sulfate}$ (n = 219, Fig. 6). The plot revealed a linear negative relationship (4) between them:

$$\delta^{18}O_{sulfate} = -2.277 \times \log_e(SO_4{}^{2-}) + 1.386 \pm 5 \tag{4}$$

where sulfate concentration is in mmol l^{-1} and $\delta^{18}O_{sulfate}$ is in per mil.

The $\delta^{18}O_{sulfate}$ of leachate from the waste rock dump at the Sangdeok mine was very low (−4.6‰) and this $\delta^{18}O_{sulfate}$ value was plotted markedly below the regression line. Relevant $\delta^{18}O_{H2O}$ were not analyzed for the surveys, but reported isotopic values vary between −6 and −8‰ in coastal groundwater in the eastern part of South Korea (Kim et al., 2014). The altitude effect of water oxygen was reported to be about −0.28‰ per 100 m (Poage and Chamberlain, 2001), and the

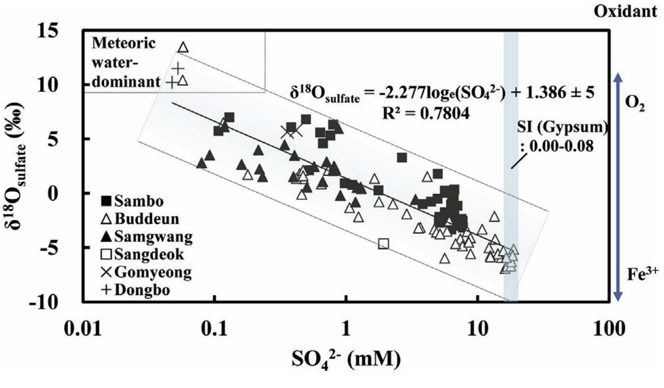

Fig. 6. Relationship between sulfate concentration and $\delta^{18}O_{sulfate}$ from the samples (n = 219) from regional and MLS surveys. Range of meteoric water reported by Yu et al. (2007) was also indicated.

altitude of Sangdeok mine is 900–1000 m above sea level (highest among the six mines) which can decrease $\delta^{18}O_{H2O}$ by about −2.2 to −2.8‰ and may explain the lower $\delta^{18}O_{sulfate}$ in the Sangdeok mine than the regression line. The maximum difference of altitude among mine areas was ~900 m (between 1000 m in the Sangdeok mine and 100 m in the Sambo mine), from which a topographic effect of about 2.5‰ can be derived. Evaporation during the reaction of intermediate species is not supposed to significantly affect the $\delta^{18}O$ value of water and hence those of sulfate generated in these waters ($\delta^{18}O_{sulfate}$), because intermediate sulfur species forming between sulfide and sulfate have short residence time (e.g. Zhang and Millero, 1991; Müller et al., 2013). In addition, the oxygen isotopic exchange rate of dissolved sulfate and ambient water is extremely slow at environmental temperatures and pH values. For example, even in the environment of pH 4, the half-time of oxygen exchange between sulfate and water is of the order of 1000 years (Lloyd, 1967). Thus incorporation and/or exchange of oxygen after formation of sulfate were not considered to occur downstream.

The upper limit of sulfate concentration in the samples should be controlled by the saturation of gypsum. Because the Ca concentration showed a good linear relationship with sulfate in the mine-affected environments with circum-neutral pH (Kim et al., 2017), increasing concentrations of sulfate should result in increased concentrations of Ca and eventually saturation of gypsum. Two water samples with the highest sulfate and Ca concentrations revealed slightly positive SI with respect to gypsum (0.08 and 0.06 for 30 m depth at MLS2 and 24.5 m depth at MLS1 in Buddeun mine in July, respectively), as the result of geochemical modeling by PHREEQC (see Table S1 of Supplementary Information). Also, the range of the highest sulfate concentrations (15.73–18.79 mM) coincided with the SI of 0.00–0.08 (Fig. 6), which is similar with the SI values (0.01–0.04) reported by Smuda et al. (2008). Thus, the maximum sulfate concentration of the samples in the mining areas is restricted by saturation and precipitation of secondary gypsum.

According to the reactions (1) and (3), oxygen isotopic composition of sulfate can be calculated using the isotopic mixing equation (Lloyd, 1967):

$$\delta^{18}O_{sulfate} = X\,(\delta^{18}O_{H2O} + \varepsilon^{18}_{sulfate\text{-}H2O}) + (1 - X)\,(\delta^{18}O_{O2} + \varepsilon^{18}_{sulfate\text{-}O2}) \tag{5}$$

where X is the relative proportion of water-derived oxygen in sulfate. Reported $\delta^{18}O_{H2O}$ vary between −6 and −8‰ in a coastal groundwater system in the eastern part of South Korea (Kim et al., 2014) and would decrease to −9 to −11‰ by the altitude effect (about −3‰), resulting in an entire range between −6 and −11‰ (−8.5 ± 2.5‰). $\varepsilon^{18}O_{sulfate\text{-}H2O}$ range between 0.0 and 4.1‰ (2.05 ± 2.05‰) based on several studies [0.0‰ from Taylor and Wheeler (1994); 2.05 ± 2.05‰ from Taylor et al. (1984b); 2.3‰ from Heidel and Tichomirowa (2011a); 2.6‰ from van Everdingen and Krouse (1985) and Mazumdar et al. (2008); 3 ± 1‰ from Toran and Harris (1989); 3.4 ± 0.6‰ from Balci et al. (2007)]. Among them, biological and abiotic condition did not result in a significant difference in oxygen isotope fractionation between sulfate and water (Balci et al., 2007). Kroopnick and Craig (1972) reported a $\delta^{18}O$ value of atmospheric oxygen of 23.5 ± 0.3‰. Enrichment factors between dissolved sulfate and molecular oxygen ($\varepsilon^{18}O_{sulfate\text{-}O2}$) were previously reported as −8.7‰ (Lloyd, 1967), −9.8‰ (Heidel and Tichomirowa, 2010), −10.3 ± 0.5‰ (Balci et al., 2007) and −11.4‰ (Taylor et al., 1984b), hence overall ranging between −8.7 and −11.4‰ (−10.05 ± 1.35‰).

Taylor et al. (1984b) investigated varying proportions of water oxygen in sulfate from oxidation of pyrite at pH of 2.0 with or without *Thiobacillus ferrooxidans*, and reported water-derived oxygen constituted between 23 and 100% of the oxygen in the sulfate. Gould et al. (1989) also conducted experiments for oxidation of sulfide minerals (pyrite, sphalerite, chalcopyrite and pentlandite) under acidic condition (pH 2.5) with *A. ferrooxidans*. The percentage of water oxygen was 23–80% for all their samples and 66–71% for pyrite. In addition, Toran (1987), Krouse and Mayer (2000), Taylor et al. (1984b), Balci et al. (2007), Taylor and Wheeler (1994), van Stempvoort and Krouse (1994), Tichomirowa and Junghans (2009) and Kohl and Bao (2011) reported that between 40 and 100% of water oxygen was incorporated in sulfate from sulfide oxidation. Especially for field studies, van Everdingen and Krouse (1988), Taylor et al. (1984a), and van Everdingen et al. (1985) reported a wide range of H_2O-derived oxygen (X) in sulfate (about 25–90%). Thus, the reported overall range for X is between 23 and 100%. From equation (5) and suggested ranges of parameters above, $\delta^{18}O_{sulfate}$ should be as high as 8.9 ± 2.3‰ (6.6–11.2‰) if 23% of oxygen in sulfate is derived from water oxygen (X = 0.23), and may be as low as −6.5 ± 4.6‰ (−11.0 to −1.9‰) in the case of X = 1.00. These predicted ranges agree well with the range of observed $\delta^{18}O_{sulfate}$ values plotted in Fig. 6 except for water samples with sulfate dominated by meteoric water. Heidel and Tichomirowa (2011a) observed varying $\delta^{18}O_{sulfate}$ values according to various conditions for Fe(III)/pyrite-surface, from $\delta^{18}O_{sulfate}$ of +6.9 to +7.4‰ at Fe(III)/pyrite-surface of 0.001 mmol m^{-2}, to −7.5‰ at Fe(III)/pyrite-surface of 13.6 mmol m^{-2} ($\delta^{18}O_{H2O}$ was −8.9‰). A negative linear regression line between $\delta^{18}O_{sulfate}$ and logarithm of Fe(III)/pyrite-surface ratio was established (data not presented) based on the data of Heidel and Tichomirowa (2011a) with a $\delta^{18}O_{H2O}$ of −8.9‰, and it had a coefficient of determination of 0.872 (n = 16). This suggests that the amount of Fe(III) in specific environment controls in part the proportion of water-derived oxygen in the newly formed sulfate. These authors also suggested that initial preferential consumption of adsorbed molecular oxygen lead to stronger contribution of dissolved molecular oxygen until its depletion. So they reported considerable contribution of molecular oxygen up to ~71% in environment with limited ferric iron even at low pH (~2.0), although Taylor et al. (1984a,b) and Balci et al. (2007) indicated water-derived oxygen and ferric iron as oxidant are more important at least at low pH. In addition, Heidel and Tichomirowa (2011a and references therein), Balci et al. (2007), Heidel et al. (2011), Gould et al. (1989), Tichomirowa and Junghans (2009), Kohl and Bao (2011), Reedy et al. (1991), Yu et al. (2001), Brunner et al. (2008), and Heidel et al. (2013) indicated that prolonged oxidation leads to simultaneous increase of sulfate and contribution from water oxygen, while molecular oxygen tends to be incorporated into sulfate from a shorter duration of pyrite oxidation. Our survey covering background as well as mine-affected downstream waters in six mines was expected to include samples which lack ferric iron and reaction time required for sulfide oxidation, so incorporation of dissolved oxygen may be considerable for those. Measured data of DO, Fe^{2+} and Fe^{3+} are available in Table S2 of the Supplementary Information.

The lowest concentrations (< 0.1 mM) of sulfate found in four samples from the Buddeun and Dongbo mines fell between those of atmospheric deposition in Chuncheon of Gangwon province, Korea (2.1×10^{-3} to 0.25 mM; Yu et al., 2007), and deviated considerably from the regression plotting above the line. The reported $\delta^{18}O_{sulfate}$ range of the meteoric water was 9.0–16.6‰, coinciding with higher $\delta^{18}O_{sulfate}$ of four samples when compared with the regression line. Thus, the lower limit of sulfate concentration can be defined by the occurrence of dissolved sulfate from atmospheric input.

Sulfite has been reported to exchange its oxygen with ambient water and the rate of exchange depends on pH, sulfite concentration and temperature (Betts and Voss, 1970; Holt et al., 1981; Krouse et al., 1991; Zhang and Millero, 1991; Hubbard et al., 2009; Müller et al., 2013). The sulfite can further be oxidized by either dissolved oxygen (Holt et al., 1981, 1983) or ferric iron (Brandt and van Eldik, 1998; Millero, 2001). Thus the oxygen exchange between sulfite and ambient water might also affect the oxygen in sulfate oxygen. However, Kohl and Bao (2011) and Müller et al. (2013) reported that oxygen isotope exchange was not significant at acidic to neutral pH because sulfite oxidation rates out-competed exchange rates. Even if most of the samples in our study had circum-neutral pH, they may have had low "initial" pH between 1.46 and 3.98 with average of 2.49 (according to the stoichiometry of generated protons from equation (1) and sulfate concentrations) at the time of sulfate generation before neutralization by carbonates and/or silicates (Kim et al., 2017). This suggests that sulfite oxidation rates exceeded isotope exchange rates between sulfite and water in our study. In addition, Holt et al. (1981) suggested the enrichment factor for sulfite-water oxygen exchange ($\varepsilon^{18}_{SO3-H2O}$) of 24‰ at pH ~4.5, and Brunner et al. (2006) reported increasing $\varepsilon^{18}_{SO3-H2O}$ with decreasing pH. Thus, if the samples in our study experienced sulfite-water oxygen exchange, $\delta^{18}O_{sulfite}$ would be higher than 15.5 ± 2.5‰, and the resulting $\delta^{18}O_{sulfate}$ would be > 5.8 ± 2.8‰ and > 9.7 ± 3.2‰ after oxidation by O_2 ($\varepsilon^{18}_{SO3+O2\rightarrow SO4}$ of −9.7 ± 0.3‰ was applied; Müller et al., 2013) or ferric iron ($\varepsilon^{18}_{SO3+H2O\rightarrow SO4}$ of −5.8 ± 0.7‰ was applied; Müller et al., 2013), respectively. Those oxygen isotope values of sulfate are too high to span the observed values. Thus, the observed $\delta^{18}O_{sulfate}$ values and sulfate concentrations indicate that the mechanism of sulfite-water oxygen exchange may not be significant for most of the samples in our study.

4. Conclusions

As a result of sulfur and oxygen isotopic investigations in six mines of South Korea, $\delta^{34}S_{sulfate}$ for the most of surface and ground water samples effectively reflected $\delta^{34}S_{sulfide}$ signature of ore sulfide minerals in mine area. The use of $\delta^{34}S_{sulfate}$ and $\delta^{18}O_{sulfate}$ together could also identify and trace contamination source containing sulfides and sulfates in mine area.

The plot between dissolved sulfate and $\delta^{18}O_{sulfate}$ for a large dataset ($n = 219$) spanning the studied six mines in South Korea showed a negative linear relationship, which implies that enhanced oxidation by ferric iron involved water-derived oxygen to incorporate into dissolved sulfate and that sulfate concentration accordingly increased exponentially. The mechanism for this is suggested to be the consumption of initial molecular oxygen at early stage, whereas prolonged oxidation resulted in higher influence of ferric iron with more oxygen from water molecules. The observed range of $\delta^{18}O_{sulfate}$ could span between the region where most of oxygen atoms are derived from molecular oxygen and the region of ~100% from water molecules. In addition, the upper and lower limit could be explained as restriction by saturation of gypsum and atmospheric input, respectively. This study based on field data confirms that the relationship between dissolved sulfate concentration and $\delta^{18}O_{sulfate}$ is very useful for semi-quantative interpretation of sulfide oxidation pathways. However, it is needed to verify the relationship by additional studies in the other mine areas. In addition, further investigations are needed to reveal the origin and relevant mechanism of $\delta^{34}S_{sulfate}$-depleted deep groundwater.

Acknowledgments

This work was supported by the Mine Reclamation Corporation (MIRECO) funded by the Ministry of Trade, Industry and Energy. Completion of this work was partly supported by Korea Environment Industry & Technology Institute (KEITI) through Subsurface Environment Management (SEM) Project, funded by Korea Ministry of Environment. Yuri Cho and many students at Environmental Geochemistry Laboratory in Korea University, Professor Man Sik Choi and his students at Chemical Oceanography Laboratory in Chungnam University, and Ji-Hye Hong at the MIRECO helped the authors in well installation, field works and data preparation. Constructive comments provided by anonymous reviewers helped to clarify and improve the manuscript.

Appendix A. Supplementary data

Supplementary data to this article can be found online at https://doi.org/10.1016/j.apgeochem.2018.11.018.

References

Balci, N., Shanks III, W.C., Mayer, B., Mandernack, K.W., 2007. Oxygen and sulfur isotope systematics of sulfate produced by bacterial and abiotic oxidation of pyrite. Geochem. Cosmochim. Acta 71, 3796–3811.

Balci, N., Mayer, B., Shanks III, W.C., Mandernack, K.W., 2012. Oxygen and sulfur isotope systematics of sulfate produced during abiotic and bacterial oxidation of sphalerite and elemental sulfur. Geochem. Cosmochim. Acta 77, 335–351.

Betts, R.H., Voss, R.H., 1970. The kinetics of oxygen exchange between sulfite ion and water. Can. J. Chem. 48, 2035–2041.

Bottrell, S.H., 2007. Stable isotopes in aqueous sulphate as tracers of natural and contaminant sulphate sources: a reconnaissance study of the Xingwen karst aquifer, Sichuan, China. In: Parise, M., Gunn, J. (Eds.), Natural and Anthropogenic Hazards in Karst Areas: Recognition, Analysis and Mitigation. vol. 279. Geological Society London, Special Pub, pp. 123–135.

Brandt, C., van Eldik, R., 1998. Kinetics and mechanism of the iron(III)-catalyzed autooxidation of sulfur(IV) oxides in aqueous solution - the influence of pH, medium and aging. Transit. Met. Chem. 23, 667–675.

Brunner, B., Mielke, R.E., Coleman, M., 2006. Abiotic Oxygen Isotope Equilibrium Fractionation between Sulfite and Water. Eos Trans. AGU 87 Fall Meet. Abstract V11C–0601.

Brunner, B., Yu, J.Y., Mielke, R.E., MacAskill, J.A., Madzunkov, S., McGenity, T.J., Coleman, M., 2008. Different isotope and chemical patterns of pyrite oxidation related to lag and exponential growth phases of *Acidithiobacillus ferrooxidans* reveal a microbial growth strategy. Earth Planet Sci. Lett. 270, 63–72.

Butler, T.W., 2007. Isotope geochemistry of drainage from an acid mine impaired watershed, Oakland, California. Appl. Geochem. 22, 1416–1426.

Clark, I.D., Fritz, P., 1997. Environmental Isotopes in Hydrogeology. Lewis Publishers, New York.

Cline, J.D., 1969. Spectrophotometric determination of hydrogen sulfide in natural waters. Limnol. Oceanogr. 14, 454–458.

Coleman, M.L., Moore, M.P., 1978. Direct reduction of sulfates to sulfur dioxide for isotopic analysis. Anal. Chem. 50, 1594–1595.

Coplen, T.B., Hopple, J.A., Böhlke, J.K., Peiser, H.S., Rieder, S.E., Krouse, H.R., Rosman, K.J.R., Ding, T., Vocke, R.D., Revesz, K.M., Lamberty, A., Taylor, P., de Bievre, P., 2002. Compilation of minimum and maximum isotope ratios of selected elements in naturally occurring terrestrial materials and reagents. U.S. Geol. Surv. Water-Resour. Invest. Rep 01–4222, 98p.

Dold, B., Spangenberg, J.E., 2005. Sulfur speciation and stable isotope trends of water-soluble sulfates in mine tailings profiles. Environ. Sci. Technol. 39, 5650–5656.

Field, C.W., 1966. Sulfur isotopic method for discriminating between sulfates of hypogene and supergene origin. Econ. Geol. 61, 1428–1435.

Gammons, C.H., Duaime, T.E., Parker, S.R., Poulson, S.R., Kennelly, P., 2010. Geochemistry and stable isotope investigation of acid mine drainage associated with abandoned coal mines in central Montana, USA. Chem. Geol. 269, 100–112.

Gammons, C.H., Brown, A., Poulson, S.R., Henderson, T.H., 2013. Using stable isotopes (S, O) of sulfate to track local contamination of the Madison karst aquifer, Montana, from abandoned coal mine drainage. Appl. Geochem. 31, 228–238.

Gonfiantini, R., Stichler, W., Rozanski, K., 1995. Standards and intercomparison materials distributed by the International Atomic Energy Agency for stable isotope measurements. In: Staff, I. (Ed.), Reference and Intercomparison Materials for Stable Isotopes of Light Elements. International Atomic Energy Agency, pp. 13–29.

Gould, W.D., McCready, R.G.L., Rajan, S., Krouse, H.R., 1989. Stable isotope composition of sulphate produced during bacterial oxidation of various metal sulphides. In: Biohydrometallurgy –Proceedings of the International Symposium (Jackson Hole, Wyoming, August 13–18), CANMET Report SP89-10, Miner. Metal. Mater. Soc, pp. 81–91.

Haur, A., Hladikova, J., Smejkal, V., 1973. Procedure of direct conversion of sulfates into SO_2 for mass spectrometric analysis of sulfur. Isotopenpraxis 18, 433–436.

Heidel, C., Tichomirowa, M., 2010. The role of dissolved molecular oxygen in abiotic pyrite oxidation under acid pH conditions – experiments with ^{18}O-enriched molecular oxygen. Appl. Geochem. 25, 1664–1675.

Heidel, C., Tichomirowa, M., 2011a. The isotopic composition of sulfate from anaerobic and low oxygen pyrite oxidation experiments with ferric iron – new insights into oxidation mechanisms. Chem. Geol. 281, 305–316.

Heidel, C., Tichomirowa, M., 2011b. Galena oxidation investigations on oxygen and sulphur isotopes. Isot. Environ. Health Stud. 47, 169–188.

Heidel, C., Tichomirowa, M., Breitkopf, C., 2011. Sphalerite oxidation pathways detected by oxygen and sulfur isotope studies. Appl. Geochem. 26, 2247–2259.

Heidel, C., Tichomirowa, M., Junghans, M., 2013. Oxygen and sulfur isotope investigations of the oxidation of sulfide mixtures containing pyrite, galena, and sphalerite. Chem. Geol. 342, 29–43.

Hoefs, J., 2004. Stable Isotope Geochemistry. Springer-Verlag, Berlin.

Holser, W.T., Kaplan, I.R., 1966. Isotope geochemistry of sedimentary sulfates. Chem. Geol. 1, 93–135.

Holt, B.D., Engelkemeier, A.G., 1970. Thermal decomposition of barium sulfate to sulfur dioxide for mass spectrometric analysis. Anal. Chem. 42, 1451–1453.

Holt, B.D., Kumar, R., Cunningham, P.T., 1981. Oxygen-18 study of the aqueous-phase oxidation of sulfur dioxide. Atmos. Environ. 15, 557–566.

Holt, B.D., Cunningham, P.T., Engelkemeir, A.G., Graczyk, D.G., Kumar, R., 1983. Oxygen-18 study of the nonaqueous-phase oxidation of sulfur dioxide. Atmos. Environ. 17, 625–632.

Hubbard, C.G., Black, S., Coleman, M.L., 2009. Aqueous geochemistry and oxygen isotope compositions of acid mine drainage from the Río Tinto, SW Spain, highlight inconsistencies in current models. Chem. Geol. 265, 321–334.

Jeong, C.H., Koh, Y.K., Kim, S.J., Kim, C.S., 1995. Hydrogeochemistry and water-rock interaction in the gneiss of the Samkwang mine area. J. Geol. Soc. Korea 31, 91–105.

Junghans, M., Tichomirowa, M., 2009. Using sulfur and oxygen isotope data for sulfide oxidation assessment in the Freiberg polymetallic sulfide mine. Appl. Geochem. 24, 2034–2050.

Killingsworth, B.A., Bao, H., Kohl, I.E., 2018. Assessing pyrite-derived sulfate in the Mississippi River with four years of sulfur and triple-oxygen isotope data. Environ. Sci. Technol. 52, 6126–6136.

Kim, K.H., Mizutani, Y., Moon, H.S., 1995. Oxygen and sulfur isotopic compositions of quartz, barite and sulfide minerals from the Sambo Pb-Zn-barite ore deposits, South Korea. Geochem. J. 29, 277–286.

Kim, D.M., Yun, S.T., Kwon, M.J., Mayer, B., Kim, K.H., 2014. Assessing redox zones and seawater intrusion in a coastal aquifer in South Korea using hydrogeological, chemical and isotopic approaches. Chem. Geol. 390, 119–134.

Kim, D.M., Yun, S.T., Cho, Y., Hong, J.H., Batsaikhan, B., Oh, J., 2017. Hydrochemical assessment of environmental status of surface and ground water in mine areas in South Korea: emphasis on geochemical behaviors of metals and sulfate in ground water. J. Geochem. Explor. 183, 33–45.

Kim, S.H., Yun, S.T., Kweon, S.H., Lee, D.H., 1994. Epithermal gold - silver mineralization of the Dongbo mine. J. Kor. Soc. Geosys. Eng. 31, 355–363.

Kohl, I., Bao, H., 2011. Triple-oxygen-isotope determination of molecular oxygen incorporation in sulfate produced during abiotic pyrite oxidation (pH = 2–11). Geochem. Cosmochim. Acta 75, 1785–1798.

Kroopnick, P., Craig, H., 1972. Atmospheric oxygen: isotopic composition and solubility fractionation. Science 175, 54–55.

Krouse, H.R., Mayer, B., 2000. Sulphur and oxygen isotopes in sulphate. In: Cook, P.G., Herczeg, A.L. (Eds.), Environmental Tracers in Subsurface Hydrology. Kluwer Academic, pp. 195–231.

Krouse, H.R., Gould, W.D., McCready, R.G.L., Rajan, S., 1991. ^{18}O incorporation into sulphate during the bacterial oxidation of sulphide minerals and the potential for oxygen isotope exchange between O_2, H_2O and oxidized sulphur intermediates. Earth Planet Sci. Lett. 107, 90–94.

Lee, H.K., Yoo, B.C., Kim, K.W., Choi, S.G., 1998. Mode of occurrence and chemical composition of electrums from the Samkwang gold-silver deposits, Korea. J. Kor. Soc. Geosys. Eng. 35, 8–18.

Lee, J.H., Hueley, P.M., 1973. U-pb Zircon Age of the Precambrian Basement Gneisses of South Korea. Geology and Ore Deposit No. 21. Geological and Mineral Institute of Korea.

Lloyd, R.M., 1967. Oxygen-18 composition of oceanic sulphate. Science 156, 1228–1231.

Lloyd, R.M., 1968. Oxygen isotope behavior in the sulfate-water system. J. Geophys. Res. 73, 6099–6110.

Mayer, B., 2005. Assessing sources and transformations of sulphate and nitrate in the hydrosphere using isotope techniques. In: Aggarwal, P.K., Gat, J.R., Froehlich, K.F.O. (Eds.), Isotopes in the Water Cycle: Past, Present and Future of a Developing Science. IAEA, Netherlands, pp. 67–89.

Mazumdar, A., Goldberg, T., Strauss, H., 2008. Abiotic oxidation of pyrite by Fe(III) in acidic media and its implications for sulfur isotope measurements of lattice-bound sulfate in sediments. Chem. Geol. 253, 30–37.

Migaszewski, Z.M., Gałuszka, A., Dołęgowska, S., 2018. Stable isotope geochemistry of acid mine drainage from the Wiśniówka area (south-central Poland). Appl. Geochem. 95, 45–56.

Millero, F.J., 2001. The Physical Chemistry of Natural Waters. Wiley Interscience, New York, pp. 654.

MIRECO (Korea Mine Reclamation Corp), 2009. Detailed Survey on Remediation of Contaminated Soil in Gomyeong-dongbo Mine. MIRECO, Seoul, Korea (in Korean).

Moon, K.J., 1986. Study on the temperature and the origin of mineralization at the Samkwang Au deposits. J. Korean Inst. Min. Geol. 19, 19–24.

Müller, I.A., Brunner, B., Coleman, M., 2013. Isotopic evidence of the pivotal role of sulfite oxidation in shaping the oxygen isotope signature of sulfate. Chem. Geol. 354, 186–202.

Nordstrom, D.K., Alpers, C.N., 1999. Geochemistry of acid mine waters. In: Plumlee, G.D., Logsdon, M.J. (Eds.), The Environmental Geochemistry of Mineral Deposits. Part A: Processes, Techniques, and Health Issues. Soc. Econ. Geol.

Nordstrom, D.K., Wright, W.G., Mast, M.A., Bove, D.J., Rye, R.O., 2007. Aqueous-sulfate stable isotopes – a study of mining-affected and undisturbed acidic drainage. U. S. Geol. Surv. Prof. Pap. 1651, 387–416.

Park, H.I., Choi, S.W., Lee, S.S., 1988. Gold and silver mineralization of the Pungjeong vein, Dadeok mine. J. Korean Inst. Min. Geol. 3, 269–276.

Parkhurst, D.L., Appelo, C.A.J., 2015. PHREEQC (Version 3) – a Computer Program for Speciation, Batch-reaction, One-dimensional Transport, and Inverse Geochemical Calculations. United States Geological Survey (USGS).

Poage, M.A., Chamberlain, C.P., 2001. Empirical relationships between elevation and the stable isotope composition of precipitation and surface waters: considerations for studies of paleoelevation change. Am. J. Sci. 301, 1–15.

Raab, M., Spiro, B., 1991. Sulfur isotopic variations during seawater evaporation with fractional crystallization. Chem. Geol. 86, 323–333.

Reedy, B.J., Beattie, J.K., Lowson, R.T., 1991. A vibrational spectroscopic ^{18}O tracer study of pyrite oxidation. Geochem. Cosmochim. Acta 55, 1609–1614.

Samborska, K., Halas, S., 2010. ^{34}S and ^{18}O in dissolved sulfate as tracers of hydrogeochemical evolution of the Triassic carbonate aquifer exposed to intense groundwater exploitation (Olkusz-Zawiercie region, southern Poland). Appl. Geochem. 25, 1397–1414.

Singer, P.C., Stumm, W., 1970. Acid mine drainage: the rate-limiting step. Science 167, 1121–1123.

Smuda, J., Dold, B., Spangenberg, J.E., Pfeifer, H.-R., 2008. Geochemistry and stable isotope composition of fresh alkaline porphyry copper tailings: implications on sources and mobility of elements during transport and early stages of deposition. Chem. Geol. 256, 62–76.

So, C.S., Park, M.E., Shelton, K.L., Seidemann, D.E., 1984. Geology and geochemistry of the Sambo Pb-Zn deposit, Republic of Korea. Econ. Geol. 79, 656–670.

Sun, J., Kobayashi, T., Strosnider, W.H.J., Wu, P., 2017. Stable sulfur and oxygen isotopes as geochemical tracers of sulfate in karst waters. J. Hydrol. 551, 245–252.

Taylor, B.E., Wheeler, M.C., 1994. Sulfur- and oxygen- isotope geochemistry of acid mine drainage in the western United States. In: Alpers, C.N., Blowes, D.W. (Eds.), Environmental Geochemistry of Sulfide Oxidation. vol. 550. American Chemical Society Symposium Series, pp. 481–514.

Taylor, B.E., Wheeler, M.C., Nordstrom, D.K., 1984a. Isotope composition of sulphate in acid mine drainage as measure of bacterial oxidation. Nature 308, 538–541.

Taylor, B.E., Wheeler, M.C., Nordstrom, D.K., 1984b. Stable isotope geochemistry of acid mine drainage: experimental oxidation of pyrite. Geochem. Cosmochim. Acta 48, 2669–2678.

Thode, H.G., Monster, J., 1965. Sulfur-isotope geochemistry of petroleum, evaporites, and ancient seas, fluids in subsurface environments. In: Fluids in Subsurface Environments, Memoir 4. Am. Assoc. Petrol. Geol., pp. 367–377.

Tichomirowa, M., Junghans, M., 2009. Oxygen isotope evidence for sorption of molecular oxygen to pyrite surface sites and incorporation into sulfate in oxidation experiments. Appl. Geochem. 24, 2072–2092.

Toran, L., 1987. Sulfate contamination in groundwater from a carbonate-hosted mine. J. Contam. Hydrol. 2, 1–29.

Toran, L., Harris, R.F., 1989. Interpretation of sulfur and oxygen isotopes in biological and abiological sulfide oxidation. Geochem. Cosmochim. Acta 53, 2341–2348.

Thurston, R.S., Mandernack, K.W., Shanks III, W.C., 2010. Laboratory chalcopyrite oxidation by *Acidithiobacillus ferrooxidans*: oxygen and sulfur isotope fractionation. Chem. Geol. 269, 252–261.

Tuttle, M.L.W., Breit, G.N., Cozzarelli, I.M., 2009. Processes affecting δ^{34}S and δ^{18}O values of dissolved sulfate in alluvium along the Canadian River, central Oklahoma, USA. Chem. Geol. 265, 455–467.

van Everdingen, R.O., Krouse, H.R., 1985. Isotope composition of sulphates generated by bacterial and abiological oxidation. Nature 315, 395–396.

van Everdingen, R.O., Krouse, H.R., 1988. Interpretation of Isotopic Compositions of Dissolved Sulfates in Acid Mine Drainage. U.S. Bureau of Mines Circular 9183: Mine Drainage and Surface Mine Reclamation. pp. 147–156.

van Everdingen, R.O., Shakur, M.A., Michel, F.A., 1985. Oxygen- and sulfur- isotope geochemistry of acidic groundwater discharge in British Columbia, Yukon, and District of Mackenzie, Canada. Can. J. Earth Sci. 22, 1689–1695.

van Stempvoort, D.R., Krouse, H.R., 1994. Controls of δ^{18}O in sulfate—review of experimental data and application to specific environments. In: Alpers, C.N., Blowes, D.W. (Eds.), Environmental Geochemistry of Sulfide Oxidation, American Chemical Society Symposium Series 550, pp. 446–480.

Yoo, B.C., Lee, H.K., Choi, S.G., 2002. Stable isotope, fluid inclusion and mineralogical studies of the Samkwang gold-silver deposits, Republic of Korea. Econ. Environ. Geol. (Korea) 35, 299–316.

Yu, J.Y., McGenity, T.J., Coleman, M.L., 2001. Solution chemistry during the lag phase and exponential phase of pyrite oxidation by *Thiobacillus ferrooxidans*. Chem. Geol. 175, 307–317.

Yu, J.Y., Park, Y., Mielke, R.E., Coleman, M.L., 2007. Sulfur and oxygen isotopic compositions of the dissolved sulphate in the meteoric water in Chuncheon, Korea. Geosci. J. 11, 357–367.

Yuan, F., Mayer, B., 2012. Chemical and isotopic evaluation of sulfur sources and cycling in the Pecos River, New Mexico, USA. Chem. Geol. 291, 13–22.

Zhang, J.-Z., Millero, F.J., 1991. The rate of sulfite oxidation in seawater. Geochem. Cosmochim. Acta 55, 677–685.

Zhang, D., Li, X.D., Zhao, Z.Q., Liu, C.Q., 2015. Using dual isotopic data to track the sources and behaviors of dissolved sulfate in the western North China Plain. Appl. Geochem. 52, 43–56.